PCCP

Cite this: *Phys. Chem. Chem. Phys.*, 2011, **13**, 18971–18975

www.rsc.org/pccp

**PAPER**

# Stark-selected beam of ground-state OCS molecules characterized by revivals of impulsive alignment

**Jens H. Nielsen,[a] Paw Simesen,[a] Christer Z. Bisgaard,[b] Henrik Stapelfeldt,*[cd] Frank Filsinger,[e] Bretislav Friedrich,[e] Gerard Meijer[e] and Jochen Küpper*[efg]**

***Received 12th April 2011, Accepted 4th July 2011***
**DOI: 10.1039/c1cp21143a**



We make use of an inhomogeneous electrostatic dipole field to impart a quantum-state-dependent deflection to a pulsed beam of OCS molecules, and show that those molecules residing in the absolute ground state, $X^1\Sigma^+$, $|00^00\rangle$, $J = 0$, can be separated out by selecting the most deflected part of the molecular beam. Past the deflector, we irradiate the molecular beam by a linearly polarized pulsed nonresonant laser beam that impulsively aligns the OCS molecules. Their alignment, monitored *via* velocity-map imaging, is measured as a function of time, and the time dependence of the alignment is used to determine the quantum state composition of the beam. We find significant enhancements of the alignment ($\langle\cos^2\theta_{2D}\rangle = 0.84$) and of state purity ($>92\%$) for a state-selected, deflected beam compared with an undeflected beam.

The ability to produce ensembles of atoms and molecules with a narrow distribution of quantum states has been a game-changer in atomic, molecular and optical physics, past and present. Recent examples from molecular physics include crossed beam scattering[1,2] and photodissociation dynamics studies at high resolution,[3] as well as the work done with and on cold and ultracold molecules.[4,5] The techniques developed to produce molecules in (nearly) single quantum states include multipole focusing,[6–10] Stark deceleration,[11,12] Zeeman deceleration[13,14]—all of which isolate molecules that are initially populated in a particular quantum state—and buffer gas cooling[15,16]—which lowers the temperature of a sample such that the resulting thermal state-distribution contains essentially only the absolute ground state. Also, photo- or magneto-association of ultracold alkali atoms can form ultracold homo- or heteronuclear diatomic molecules occupying a single electronic, vibrational and rotational state including, in certain cases, the absolute ground state.[4,5] All methods offer unique opportunities but are also subjected to limitations in terms of the type of molecules that the methods apply to or the particular quantum states that can be selected.

Here we demonstrate an alternative method, with a history reaching back to the 1920s,[17–19] to produce molecules in a single quantum state. Like multipole focusing and Stark or Zeeman deceleration it is based on selecting the molecules that are initially residing in a specific quantum state. We employ a dipolar deflection field to disperse a well-expanded, nearly monoenergetic beam of OCS molecules according to their state-specific electric dipole moments. The inhomogeneous electric field inside the deflector has an almost constant gradient over a large area surrounding the molecular beam axis and enables dispersion of the rotational quantum states of OCS. In particular, we separate out the ground rotational state, $J = 0$, of the electronic and vibrational ground state, $X^1\Sigma^+$ and $|00^00\rangle$,[20] and thereby produce a molecular beam of OCS($X^1\Sigma^+$, $|00^00\rangle$, $J = 0$) with a purity in excess of 92%. Since $^{16}O^{12}C^{32}S$ has zero nuclear spin, the ground state obtained is free of hyperfine structure. The purity of the beam was characterized by observing the time dependence of the nonadiabatic alignment[21–25] produced by the interaction of a linearly polarized nonresonant pulsed laser beam with the anisotropic OCS molecules.

In what follows, we first present an outline of the experimental setup. Then we describe the dispersion of the molecular beam achieved by the dipole deflector. The nonadiabatic alignment of the molecules and its use to characterize state purity of the molecular beam is described next. Finally, we draw conclusions from our work.

The experimental setup, detailed earlier,[26,27] is shown in Fig. 1. A pulsed molecular beam is produced by expanding a mixture of 10 bar of neon and 1 mbar of OCS into vacuum

[a] *Department of Physics and Astronomy, University of Aarhus, 8000 Aarhus C, Denmark*
[b] *Department of Photonics Engineering, Technical University of Denmark, 2800 Kgs. Lyngby, Denmark*
[c] *Department of Chemistry, University of Aarhus, 8000 Aarhus C, Denmark. E-mail: henriks@chem.au.dk*
[d] *Interdisciplinary Nanoscience Center (iNANO), University of Aarhus, 8000 Aarhus C, Denmark*
[e] *Fritz-Haber-Institut der Max-Planck-Gesellschaft, Faradayweg 4-6, 14195 Berlin, Germany. E-mail: jochen.kuepper@cfel.de*
[f] *Center for Free-Electron Laser Science, DESY, Notkestrasse 85, 22607 Hamburg, Germany*
[g] *University of Hamburg, Luruper Chaussee 149, 22761 Hamburg, Germany*

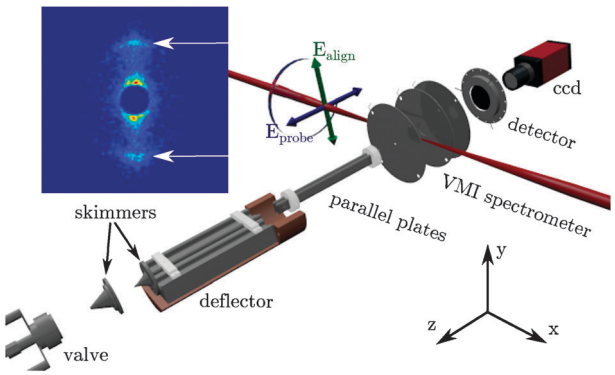


**Fig. 1** Schematic of the experimental setup. The inset shows an $S^+$ ion image recorded when the molecules are aligned along the *y*-axis ($t$ = 40.6 ps). The arrows indicate the $S^+ + CO^+$ Coulomb-explosion channel employed to determine the degree of alignment.

through a 250 μm diameter nozzle in a pulsed valve. The beam is collimated by a skimmer and sent into a 15 cm-long electrostatic deflector, which exerts a force on the molecules along the *y*-axis, *cf.* Fig. 1. After the exit of the deflector the molecules travel another 17 cm through a region between two parallel electrostatic plates (field strength: 2 kV $cm^{-1}$) to preserve a field-quantization axis before they enter into a velocity map imaging (VMI) spectrometer. Here the molecular beam is crossed by the pulsed alignment and probe laser beams propagating along the *x* axis. The laser beams, operating at a (nonresonant) wavelength of 800 nm, are focused on the molecular beam with waists ($\omega_0$) of 35 and 25 μm, respectively. The alignment pulses, linearly polarized along the *y*-axis, have a duration of 330 fs and a peak intensity of $9.6 \times 10^{12}$ W $cm^{-2}$. The duration is shorter than the rotational period, $\tau_{rot}$ = 82 ps, of OCS($X^1\Sigma^+$, $|00^00\rangle$) by about a factor of 250, ensuring that the anisotropic polarizability interaction with the molecule is nonadiabatic (in fact well within the sudden regime). The probe pulses, linearly polarized along the *z*-axis, are 30 fs long with a peak intensity of $4.8 \times 10^{14}$ W $cm^{-2}$ and ionize the molecules *via* nonresonant multiphoton absorption. The positive ions thus produced are accelerated toward an imaging detector; the 2D ion images constitute the primary data obtained in the experiment.

The effect of the deflector on the molecular beam was characterized by measuring the intensity profile of the molecular beam along the (vertical) *y* axis, see Fig. 2. This was done by recording the $OCS^+$ signal, arising from the ionization of OCS by the probe pulse as a function of the vertical position of the laser focus, see Fig. 1. When the deflector is turned off, the vertical width of the molecular beam is about 2.2 mm, mainly due to the collimation of the beam by the skimmers, which precede the deflector. When the deflector is turned on, the molecular beam profile broadens and shifts upwards, toward higher field strengths (corresponding to higher values of *y*). The molecular beam profiles were modeled by a Monte-Carlo simulation. For every relevant eigenstate of the initial OCS packet we generated a test sample of initial values of molecules in phase-space ($x$, $y$, $z$, $v_x$, $v_y$, $v_z$) and then performed (classical) trajectory simulations through the inhomogeneous electric field of the deflector. This yields a vertical beam profile for

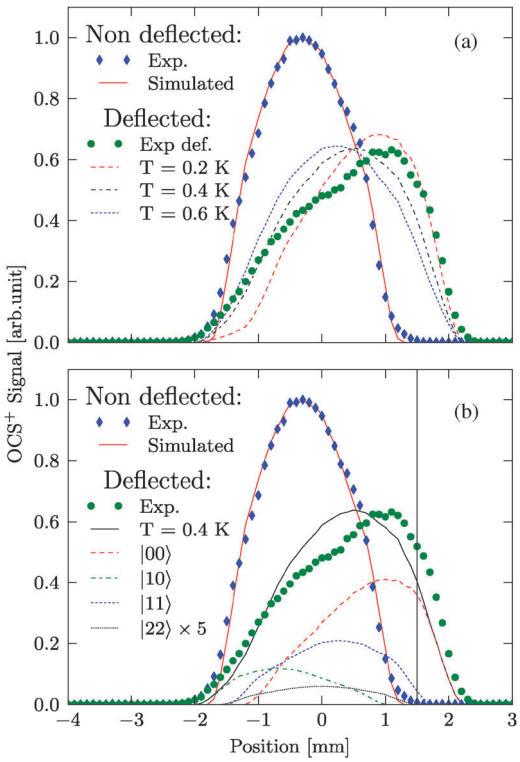


**Fig. 2** Molecular beam intensity profiles along the *y*-axis. (a) Experimental data (points) and simulated profiles (curves) for different rotational temperatures. (b) Experimental data (points) and simulated profiles (curves) at $T_{rot}$ = 0.4 K for individual rotational states. The profile for the $|22\rangle$ state is scaled up by a factor of 5. Vertical line indicates the position of the laser foci in the alignment experiment.

the given molecular quantum state. These profiles for individual states were averaged with a weight according to their populations—according to a Boltzmann distribution for different rotational temperatures $T$ of the beam and their degeneracy. In Fig. 2(a) the resulting profiles for 0.2 K, 0.4 K, and 0.6 K are given along with the experimental curve. A comparison of the measured and simulated data indicates that the $T$ = 0.4 K curve represents the experimental data best. However, a non-negligible discrepancy remains, particularly on the left tail of the deflection profile, corresponding to negative values of *y*. Likely culprits are potentially increased populations of the low-field seeking $|10\rangle$ and $|20\rangle$ states (with theoretical populations at $T$ = 0.4 K of 13% and 1.2%, respectively). This is illustrated in Fig. 2(b), which shows the Boltzmann-weighted profiles of the individual Stark states at $T$ = 0.4 K. An excess of the $|10\rangle$, $|20\rangle$ states is consistent with the experimental observations made for the impulsive alignment of OCS, described below. For the case of the temperature-independent direct (non-deflected) beam, the simulations reproduce the experimental data accurately.

Fig. 2(b) further shows that of the upward-deflected high-field-seeking states, the $|00\rangle$ state deflects the most, followed by the $|11\rangle$ state, and the $|22\rangle$ state; the low-field-seeking $|10\rangle$ state deflects downwards. At $y$ = 1.5 mm, 89% of the molecules are in the $|00\rangle$ state and 11% in the $|11\rangle$ state, while the population of the $|22\rangle$ state is negligible.

In order to characterize the quantum state composition of the deflected molecular beam, we conducted a nonadiabatic alignment experiment:[28] at time $t = 0$, the molecular beam is irradiated by an alignment pulse, see Fig. 1. The peak intensity of $9.6 \times 10^{12}$ W cm$^{-2}$ is low enough to preclude any detectable ionization of OCS. Within its focal volume, the alignment laser pulse nonadiabatically excites each molecule to a non-stationary, rotational wave packet, which undergoes periodic revivals, as does the concomitant alignment. The rotational wave packet dynamics is probed by irradiating the molecules with the probe pulse at time $t$. The probe pulse double-ionizes some of the OCS molecules, triggering their Coulomb explosion into $CO^+$ and $S^+$ ion pairs. This particular fragmentation channel can be identified by the recoil velocity as a pair of radially displaced half-rings in the outermost region of the $S^+$ ion images, such as those shown in the inset of Fig. 1.

In keeping with our previous work, we assume that the Coulomb explosion occurs rapidly enough for the axial recoil approximation to apply, in which case the emission direction of the ions is straightforwardly related to the alignment of the molecule at the instant of ionization. We quantify the alignment attained by the (experimental) degree of alignment, $\langle\cos^2\theta_{2D}\rangle$, where $\theta_{2D}$ is the angle between the velocity vector of the $S^+$ ion in the detector plane and the polarization plane of the alignment laser pulse.[29]

Fig. 3 displays the rotational wave packet dynamics, represented by the dependence of the alignment degree $\langle\cos^2\theta_{2D}\rangle$ on time over the intervals—2 ps $< t <$ 52 ps and 77 ps $< t <$ 89 ps. The two blue traces pertain to undeflected (deflector off) and the red trace to the deflected (deflector on) molecules for the laser foci placed at $y = 1.5$ mm, *cf.* Fig. 2(b). The most prominent features of the undeflected-beam trace are the prompt alignment arising shortly after the arrival (and passing) of the alignment pulse near $t = 0$, the half-period revival centered at $t = 40.6$ ps, and the first full-period revival centered at $t = 81.6$ ps.

In order to account for the observed alignment dynamics, we solved numerically the time-dependent Schrödinger equation

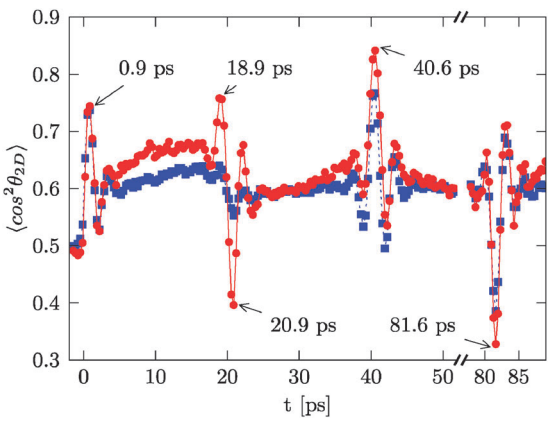


**Fig. 3** Alignment dynamics of OCS molecules, represented by the time dependence of the alignment degree, $\langle\cos^2\theta_{2D}\rangle$. The origin, $t = 0$, of the time scale is defined by the moment of arrival of the alignment pulse. Results obtained either with the direct beam or the deflected beam (at $y = 1.5$ mm) are shown, respectively, by blue squares or red circles.

for the interaction of a linearly polarized laser field with the anisotropic polarizability of the OCS molecule,[21,30] and evaluated the state-specific expectation values of the alignment cosine, $\langle\cos^2\theta\rangle_{JM}$, for each initial rotational state, $|JM\rangle$, of $^{16}O^{18}C^{32}S$. The time dependence of the alignment cosine for the $|00\rangle$, $|11\rangle$, and $|22\rangle$ states is shown in Fig. 4(a)–(c).[31] While the revival structures of the alignment cosines for the three states are similar and in phase at the half- and full-period, the revival structures at the quarter- and three-quarter-period are out of phase with respect to one another for states with opposite parity, $(-1)^J$, *i.e.*, the even-parity $|00\rangle$ and $|22\rangle$ states on the one hand and the odd-parity $|11\rangle$ state on the other. Panel (d) of Fig. 4 shows the ensemble average, $\langle\langle\cos^2\theta\rangle\rangle = \Sigma_J w_J \Sigma_M \langle\cos^2\theta\rangle_{JM}$, of the alignment cosine,[32] with $w_J$ the Boltzmann weights of the initial rotational states (these are $w_0 = 0.567$; $w_1 = 0.396$; $w_2 = 0.036$ at $T = 0.4$ K). The time dependence of $\langle\langle\cos^2\theta\rangle\rangle$ exhibits the same revival structure as the experimental dependence for the undeflected beam, blue squares in Fig. 3. In particular, the quarter and three-quarter period revivals are almost absent, due to the destructive interference of the opposite-parity contributions to $\langle\langle\cos^2\theta\rangle\rangle$ from the initial rotational states $|00\rangle$ and $|10\rangle$.

For the deflected beam (red circles in Fig. 3), the revival structure strikingly differs from that of the undeflected beam: firstly, a prominent quarter-period revival is now present. As Fig. 4(a)–(c) indicate, this can only come about if most of the

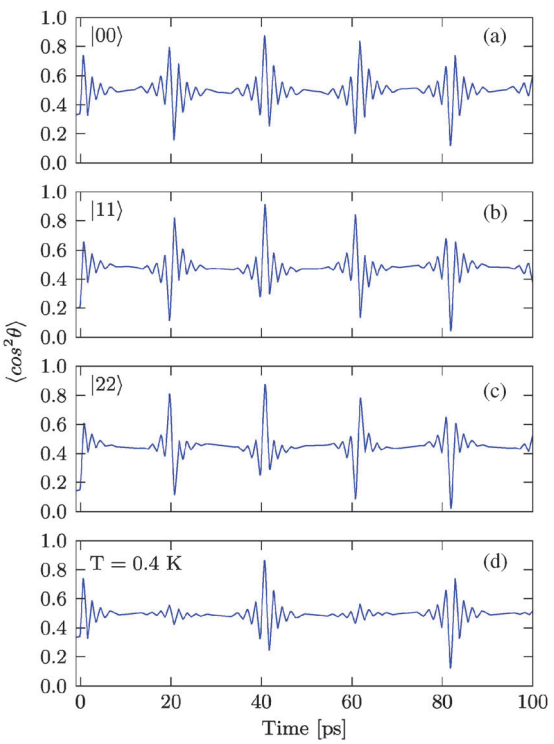


**Fig. 4** Panels (a)–(c) show the time dependence of the alignment cosine, $\langle\cos^2\theta\rangle_{JM}$, of OCS calculated over a rotational period of the molecule for different initial rotational states $|JM\rangle$. Panel (d) shows the time dependence of the ensemble-averaged alignment cosine $\langle\langle\cos^2\theta\rangle\rangle$ of OCS at a rotational temperature $T = 0.4$ K. Focal volume averaging was accounted for by including an $I^3$ probe detection efficiency based on measurements of the intensity dependence of the ionization yield.

beam molecules have the same parity. Since the position of the local minimum of the observed quarter revival (at 20.9 ps) matches that due to the $|00\rangle$ and the $|22\rangle$ states (at 20.7 ps), but not due to the $|11\rangle$ state (at 19.7 ps), it must be the $|11\rangle$ state whose concentration in the beam has been diminished. The skewed structure with a local maximum (at 18.9 ps) followed by a local minimum (at 20.9 ps) and then another (slightly lower) local maximum (at 21.7 ps) fits the simulated $|00\rangle$ trace well but is at odds with the simulated $|22\rangle$ trace. Similarly, the shapes of the observed half- and full-period revivals resemble closely those calculated for the $|00\rangle$ but not for the $|22\rangle$ state. These observations corroborate what the simulated deflection curves, Fig. 2, have suggested, namely that the molecular beam (at $y = 1.5$ mm) is dominated by the $|00\rangle$ state.

A quantitative assessment of the fraction of the $|11\rangle$ state in the deflected beam could be obtained by comparing the amplitude of the (left) local maximum at the quarter-period revival (at 18.9 ps) to the prompt alignment maximum (at 0.9 ps). This is because, as seen in Fig. 4(b) and (c), molecules in the $|00\rangle$ or $|11\rangle$ states cause the local maximum to rise or drop, respectively, in comparison with the prompt-alignment maximum. In this way, we found that at least 92% of all the beam molecules must be in the $|00\rangle$ state to account for the observed revival amplitudes, Fig. 3. The deflection curves suggest 89% population of the $|00\rangle$, in fair agreement with the alignment revival data. We note that we do not expect the simulated deflection curves to identify the $y$ position of the molecular profile to an accuracy better than 0.1 mm. This has repercussions for our ability to precisely quantify the populations of the states. For instance, at $y = 1.6$ mm the simulations yield a 94% population of the $|00\rangle$ state. The nonadiabatic alignment experiment was only conducted at one $y$-position (1.5 mm) but the simulations [Fig. 2(b)] show that a higher ground state purity can be obtained at larger $y$-positions. This will, however, occur at the expense of molecular target density.

Our assessment of the populations of the rotational states in the beam was corroborated by yet another piece of evidence: in the absence of the alignment pulse the measured alignment degree for the undeflected beam is $\langle\cos^2\theta_{2D}\rangle = 0.50$, as it should be for an isotropic ensemble, *cf.* $\langle\cos^2\theta_{2D}\rangle$ in Fig. 3 just before the alignment pulse ($t = -1$ ps). For the deflected beam, the measured alignment degree still has the isotropic value of 0.50 or perhaps marginally smaller. This is only possible if essentially only the isotropic ground state $|00\rangle$ with $\langle\cos^2\theta_{2D}\rangle = 0.5$ is present in the deflected beam while the anisotropic states $|11\rangle$ and $|22\rangle$ with $\langle\cos^2\theta_{2D}\rangle = 0.375$ and 0.312, respectively, are nearly absent.

Secondly, the alignment trace in Fig. 3 pertaining to the deflected beam exhibits a significantly more pronounced modulation of the half- and full-period revivals than the trace for the undeflected beam. Inspection of the half-period revival reveals that the local maximum of $\langle\cos^2\theta_{2D}\rangle$, which is also the global maximum, is increased from 0.77 for the undeflected beam to 0.84 for the deflected beam. We note that we did not measure the 3/4-period revival but, according to our calculations, its local alignment maximum is well below that obtained at the 1/2-period revival. Likewise, the global minimum of $\langle\cos^2\theta_{2D}\rangle$ attained at the full-period revival ($t = 81.6$ ps, see Fig. 3) decreases from 0.39 to 0.33. This means that not only alignment but also anti-alignment, *i.e.* confinement of the molecular axis to the plane perpendicular to the polarization vector of the alignment pulse, is significantly enhanced by using the deflected, state-selected beam compared with the direct beam.

The calculations displayed in Fig. 4 predict that the alignment cosine, $\langle\cos^2\theta\rangle$, only increases from 0.86 for a 0.4 K thermal ensemble to 0.87 for a pure $|00\rangle$ state. Even for a 1 K beam, the alignment cosine is 0.85. Therefore, the much more pronounced enhancement of the alignment observed experimentally is likely due to a rotational state distribution in the direct beam which is not strictly Boltzmannian. As noted above, the measured deflection curves, Fig. 2, indicate that the direct beam contains an excess of molecules in the $|10\rangle$ and possibly also the $|20\rangle$ states. Our calculations show that the alignment of these states at the half-period revival is significantly less than the alignment of the $|00\rangle$, $|11\rangle$ and $|22\rangle$ states. As a result, an increased concentration of the $|10\rangle$ and the $|20\rangle$ states in the molecular beam would lead to a weaker alignment than for a thermal beam with a Boltzmann distribution of rotational states; such non-Boltzmann behavior of supersonic expansions is a well-known phenomenon.[33–36] Overall, the deflector is well-suited for generating molecular beams that can be particularly strongly aligned.

Selecting out rotational-ground-state molecules by electrostatic deflection will be particularly effective for species with a small moment of inertia (large rotational constant), such as many diatomic and small polyatomic molecules. Supersonic molecular beams of such species tend to have a large population of the rotational ground state. The single-quantum-state selected beam may have then an intensity of up to tens of percent of the undeflected beam. Examples include IBr, ICN, ClCN, $C_2HF$, and $CH_3I$. For larger (and heavier) polyatomics, the number of states populated increases rapidly with the moment of inertia and temperature, and thus selection of the rotational ground state, if at all feasible, will occur at the expense of a much reduced beam intensity. We note that the analysis of the detailed quantum state distribution will, in general, require more analytically-dedicated methods, like resonantly enhanced multiphoton ionization (REMPI) or laser induced fluorescence (LIF), than the rotational wave packet measurements used in the present work.

The ability to select out the absolute ground state of molecules by the deflection method has implications for several research areas: (1) laser-induced alignment will clearly benefit from a state selection by the deflector, as demonstrated here. So will orientation based on pure optical methods[37,38] as well as on the combined electrostatic and nonresonant radiative fields.[26,27,39–42] In particular, related work relying on state-selection by an electrostatic hexapole has already demonstrated that single-state molecular beams are conducive to producing tightly aligned or oriented molecules.[41,42] (2) Collision/reaction dynamics in crossed molecular beams. (3) Ground-state molecules selected out by the deflector could be efficiently optically decelerated and trapped,[43] thus opening an alternate route to trapping for molecules which cannot be, for instance, Stark-decelerated.

The work was supported by the Lundbeck Foundation, the Carlsberg Foundation and the Danish Council for Independent Research.

 

## References


1 F. J. Aoiz, J. E. Verdasco, M. Brouard, J. Klos, S. Marinakis and S. Stolte, *J. Phys. Chem. A*, 2009, **113**, 14636.
2 L. Scharfenberg, J. Klos, P. J. Dagdigian, M. H. Alexander, G. Meijer and S. Y. T. van de Meerakker, *Phys. Chem. Chem. Phys.*, 2010, **12**, 10660.
3 T. P. Rakitzis, A. J. van den Brom and M. H. M. Janssen, *Science*, 2004, **303**, 1852.
4 *Cold Molecules: Theory, Experiment, Applications*, ed. R. V. Krems, W. C. Stwalley and B. Friedrich, Taylor and Francis: CRC Press, Boca Raton, 1st edn, 2009.
5 L. D. Carr, D. DeMille, R. V. Krems and J. Ye, *New J. Phys.*, 2009, **11**, 055049.
6 H. G. Bennewitz, W. Paul and C. Schlier, *Z. Phys. A: Hadrons Nucl.*, 1955, **141**, 6.
7 S. Stolte, *Ber. Bunsen-Ges. Phys. Chem.*, 1982, **86**, 413.
8 J. Reuss, in ref. 44, ch. 11, pp. 276–292.
9 D. H. Parker and R. B. Bernstein, *Annu. Rev. Phys. Chem.*, 1989, **40**, 561.
10 S. Putzke, F. Filsinger, H. Haak, J. Küpper and G. Meijer, *Phys. Chem. Chem. Phys.*, 2011, DOI: 10.1039/c1cp20721k.
11 H. L. Bethlem, G. Berden and G. Meijer, *Phys. Rev. Lett.*, 1999, **83**, 1558.
12 S. Y. T. van de Meerakker, H. L. Bethlem and G. Meijer, *Nat. Phys.*, 2008, **4**, 595.
13 N. Vanhaecke, U. Meier, M. Andrist, B. H. Meier and F. Merkt, *Phys. Rev. A: At., Mol., Opt. Phys.*, 2007, **75**, 031402.
14 E. Narevicius, A. Libson, C. G. Parthey, I. Chavez, J. Narevicius, U. Even and M. G. Raizen, *Phys. Rev. A: At., Mol., Opt. Phys.*, 2008, **77**, 051401.
15 J. Weinstein, R. deCarvalho, T. Guillet, B. Friedrich and J. Doyle, *Nature*, 1998, **395**, 921.
16 L. D. van Buuren, C. Sommer, M. Motsch, S. Pohle, M. Schenk, J. Bayerl, P. W. H. Pinkse and G. Rempe, *Phys. Rev. Lett.*, 2009, **102**, 033001.
17 H. Kallmann and F. Reiche, *Z. Phys.*, 1921, **6**, 352.
18 E. Wrede, *Z. Phys.*, 1927, **44**, 261.
19 O. Stern, *Z. Phys.*, 1926, **39**, 751.
20 The notation $|00^00\rangle$ refers to the quantum numbers for three normal vibrational modes: asymmetric stretch, bending (double degenerate, therefore $0^0$) and symmetric stretch.
21 J. Ortigoso, M. Rodriguez, M. Gupta and B. Friedrich, *J. Chem. Phys.*, 1999, **110**, 3870.
22 T. Seideman, *Phys. Rev. Lett.*, 1999, **83**, 4971.
23 F. Rosca-Pruna and M. J. J. Vrakking, *Phys. Rev. Lett.*, 2001, **87**, 153902.
24 H. Stapelfeldt and T. Seideman, *Rev. Mod. Phys.*, 2003, **75**, 543.
25 V. Loriot, P. Tzallas, E. P. Benis, E. Hertz, B. Lavorel, D. Charalambidis and O. Faucher, *J. Phys. B: At., Mol. Opt. Phys.*, 2007, **40**, 2503.
26 F. Filsinger, J. Küpper, G. Meijer, L. Holmegaard, J. H. Nielsen, I. Nevo, J. L. Hansen and H. Stapelfeldt, *J. Chem. Phys.*, 2009, **131**, 064309.
27 L. Holmegaard, J. H. Nielsen, I. Nevo, H. Stapelfeldt, F. Filsinger, J. Küpper and G. Meijer, *Phys. Rev. Lett.*, 2009, **102**, 023001.
28 An alternative method, more in line with how quantum state distributions are normally characterized, would be to use resonant multiphoton ionization or laser induced fluorescence. For OCS we did not possess the experimental setup needed to conduct such measurements whereas the fs pump–probe setup, used in the nonadiabatic experiment, was immediately available.
29 The polarization of the alignment pulse is perpendicular to the static electric field inside the VMI spectrometer. Thus, only alignment and not orientation is expected. This may change if the polarization of the alignment pulse is turned parallel to the static electric field—see ref. 41 and 45.
30 C. Z. Bisgaard, S. S. Viftrup and H. Stapelfeldt, *Phys. Rev. A: At., Mol., Opt. Phys.*, 2006, **73**, 053410.
31 Note that the calculated alignment cosine $\langle\cos^2\theta\rangle$ is different from the experimentally measured $\langle\cos^2\theta_{2D}\rangle$ but simulations have shown that their time-evolution quantitatively agrees.
32 B. Friedrich, *Eur. Phys. J. D*, 2006, **38**, 209.
33 S. Stolte, in ref. 44, ch. 25, pp. 631–652.
34 Y. R. Wu and D. H. Levy, *J. Chem. Phys.*, 1989, **91**, 5278.
35 V. Aquilanti, D. Ascenzi, M. Vitores, F. Pirani and D. Cappelletti, *J. Chem. Phys.*, 1999, **111**, 2620.
36 L. Vattuone, L. Savio, F. Pirani, D. Cappelletti, M. Okada and M. Rocca, *Prog. Surf. Sci.*, 2010, **85**, 92.
37 S. De, I. Znakovskaya, D. Ray, F. Anis, N. G. Johnson, I. A. Bocharova, M. Magrakvelidze, B. D. Esry, C. L. Cocke, I. V. Litvinyuk and M. F. Kling, *Phys. Rev. Lett.*, 2009, **103**, 153002.
38 K. Oda, M. Hita, S. Minemoto and H. Sakai, *Phys. Rev. Lett.*, 2010, **104**, 213901.
39 B. Friedrich and D. Herschbach, *J. Chem. Phys.*, 1999, **111**, 6157.
40 M. Hartelt and B. Friedrich, *J. Chem. Phys.*, 2008, **128**, 224313.
41 O. Ghafur, A. Rouzee, A. Gijsbertsen, W. K. Siu, S. Stolte and M. J. J. Vrakking, *Nat. Phys.*, 2009, **5**, 289.
42 A. Rouzee, A. Gijsbertsen, O. Ghafur, O. Shir, T. Back, S. Stolte and M. Vrakking, *New J. Phys.*, 2009, **11**, 105040.
43 R. Fulton, A. Bishop, M. Shneider and P. Barker, *Nat. Phys.*, 2006, **2**, 465.
44 *Atomic and molecular beam methods*, ed. G. Scoles, Oxford University Press, New York, NY, USA, 1988, vol. 1.
45 L. Cai, J. Marango and B. Friedrich, *Phys. Rev. Lett.*, 2001, **86**, 775.